INTERFACIAL PROPERTIES OF LIGNITE, GRAPHITE, KAOLIN, AND PYRITE

S.H. Chiang, Alec Richardson, Anni Wong

Chemical/Petroleum Engrng. Dept., University of Pittsburgh
Pittsburgh, PA 15261

This project consists of four major experiments, in which the surface/interfacial and adsorption properties, particle size, and specific surface area of Lignite (35-, 200-, and 400-mesh), Graphite Powder, Kaolin, and Pyrite, are measured. The first two experiments are minor and yield preliminary results that are combined with later results for specific purposes. These experiments involve measuring the external specific surface area of the six powdered samples using the BET volumetric adsorption apparatus with N_2 as the adsorbate, and measuring five average characteristic particle diameters and the particle size size distribution of these samples with the Omnicon Alpha Particle Field Image Analyzer. From these results, a correlation is determined between particle size and specific surface area. The third experiment involves obtaining the adsorption and desorption isotherms of the samples and determining the effect of pressure, temperature, particle size, and intrinsic nature of the coal mineral on these isotherms. Adsorption isotherms per unit weight and per unit surface area (in conjunction with the surface area results of the BET experiment) of adsorbent are determined with the CO_2 gravimetric spring adsorption apparatus. The relative film pressure, which is proportional to the area under the equilibrium adsorption isotherm on a semilogarithm plot, is also estimated.

Finally, the fourth experiment consists of two parts: 1) The pendant drop method, involving a water pendant drop in the presence of a $CO_2(g)$ or $CO_2(l)$ medium, in which the liquid-vapor and liquid-liquid interfacial tensions are measured as functions of CO_2 pressure (relative to its saturation pressure), temperature, and CO_2 phase used, based on the drop's physical dimensions at equilibrium. 2) The sessile drop method, involving a water sessile drop in equilibrium on a pelletized sample of the coal mineral in a $CO_2(g)$ or $CO_2(l)$ environment. In this three-phase system, the equilibrium advancing contact angle of the drop is measured as a function of CO_2 relative pressure, temperature, and CO_2 phase for each of the six samples. Then, with the preliminary particle size and surface area data, a correlation is drawn between the contact angle and particle size/intrinsic nature of the sample. Using the

contact angle and pendant drop data, the solid-vapor and solid-liquid interfacial tensions are calculated as functions of the above system parameters, using Young's equation and the thermodynamic equation of state:

$$\gamma_{sv} = \gamma_{sl} + \gamma_{lv} \cos\theta \quad 1)$$

$$\gamma_{sl} = [(\gamma_{sv})^{0.5} - (\gamma_{lv})^{0.5}]^2/[1 - 0.015(\gamma_{sv}*\gamma_{lv})^{0.5}] \quad 2)$$

Then the works of adhesion and cohesion are calculated from Dupre's relation; and the equation of Boyd and Livingston is used to calculate the equilibrium spreading coefficient, which, like the equilibrium contact angle, is a direct measure of the wetting tendency of the three-phase system under given system conditions:

$$W_{ad} = \gamma_{sv} + \gamma_{lv} - \gamma_{sl} = \gamma_{lv} (1 + \cos\theta) \quad 3)$$

$$W_{co} = 2\gamma_{lv} \quad 4)$$

$$S = \gamma_{sv} - (\gamma_{lv} + \gamma_{sl}) = W_{ad} - W_{co} \quad 5)$$

Then the contact angle and spreading coefficient data are compared for consistency. A system with incomplete wetting is characterized by a high contact angle and negative spreading coefficient at equilibrium; and one with complete wetting is reflected by a zero contact angle and a zero (or positive, indicating the effect of film pressure caused by impurities or an adsorbed vapor film) spreading coefficient. The ultimate objective of this project is to determine the effect of the system parameters (i.e. CO_2 pressure, temperature, CO_2 phase) and nature of the coal minerals (i.e. intrinsic and particle size/surface area) on the relative wettability of the three-phase system of coal mineral-water-CO_2 through an analysis of the interfacial and adsorption properties of the coal minerals.

Results, Discussion, and Conclusions

In the first experiment, involving measurement of the dispersed particle size and size distribution, it is found that all six samples agree in relative magnitude of the five characteristic diameters: Length-, Volume-, Surface-, Surface-Volume-, and Weight-Diameters (Table 1). Pyrite has the largest average diameter of the six samples in all five categories, with the values of 16.9, 30.6, 23.5, 52.7, and 72.5 um, respectively. The sample with the smallest overall particle size is 400-mesh Lignite, with the respective values of 7.5, 12.4, 9.7, 20.6, and 31.1 um. The sizes of the other four samples fall within the ranges of these extreme values. The order of average particle size, from largest to smallest, is determined to be: Pyrite, 35-mesh Lignite, Graphite Powder, Kaolin, 200-mesh Lignite, and 400-mesh Lignite. As expected among the Lignite samples, the 35-mesh sample has the largest particle size; and 400-mesh has the smallest. Prior to this project, the 35-mesh sample is

already provided; and the 200- and 400-mesh samples are prepared by grinding the 35-mesh particles over a controlled time period. Thus, it is concluded that the initial preparation of these samples is successful.

The weight percent and number percent particle size distributions, based on Gaussian and log-normal distribution theory, are also calculated and agree well with the results of the average particle size data. These two curves lie furthest to the right for Pyrite, indicating that the particle size distribution in the Pyrite sample is toward the largest relative sizes. Furthermore, these curves lie farthest to the left for 400-mesh Lignite; and the relative positions of the curves for all the samples agree reasonably well with the order of the average particle sizes of the six samples. The purpose of this experiment is to obtain a relative picture of the particle sizes of the samples, to compare this data with the specific surface area data from the BET experiment to determine a possible correlation, and to later use these results with the interfacial and adsorption results to determine the effect of particle size on the interfacial phenomena of the coal minerals.

From the BET volumetric N_2 adsorption experiment, it is found that Pyrite has the lowest specific surface area of all the samples: 17.4 m^2/g. In contrast, 400-mesh Lignite is found to have the highest value: 21.1. The general order of the samples, from lowest to highest surface area, is: Pyrite (17.4), 35-mesh Lignite (17.8), Graphite Powder (18.1), Kaolin (18.9), 200-mesh Lignite (19.9), and 400-mesh Lignite (21.1). This order is the exact same order as that obtained from the dispersed particle size analysis. Thus, it is concluded that an inverse relationship exists between particle size and specific surface area for the six coal minerals (Table 1). Although this is only a measure of the external (i.e. available) surface area, this relation is still valid because it is safely assumed that, as a sample is ground to smaller particle sizes, the internal surface area (which is found inside micropores) remains constant. Thus, the purpose of this test is coupled with that of the particle size test; and a further purpose is to later use the surface area results to obtain the adsorption/desorption isotherms per unit surface area of adsorbent, from the corresponding isotherm results per unit weight of adsorbent, in order to eliminate the effect of surface area (or particle size) and determine any effect of the solid sample's intrinsic nature on the adsorption properties (i.e. to determine whether adsorption is an extensive or an intensive property.

The goal of the third experiment, using the CO_2 gravimetric spring adsorption apparatus, is to measure the specific amount of CO_2 adsorbate adsorbed on the powdered sample of coal mineral (both per unit weight and unit surface area) as a function of CO_2 relative pressure and temperature for the six samples. Four temperatures (10, 15, 20, and 25°C), and the CO_2 relative pressure in increments of 20% (from 0 to 100%, based on the saturation pressure of CO_2) were tested; and each system parameter was varied independently: CO_2 pressure, temperature, and sample. The specific amount adsorbed ranged from about zero at 0% relative pressure to the order of 0.08 g/g adsorbent (at 10°C) or 0.12 g/g adsorbent (at 25°C) at 100% relative pressure for the six samples. Both the adsorption and desorption isotherms are measured, and it is found in all cases that significant hysteresis occurs, which reflects the energy lost in the adsorption-desorption cycle and hence the "irreversibility" of the process. Figures 1 and 2 show the adsorption/desorption isotherms for 35-mesh Lignite at 10 and 25°C. Similar results are obtained for the other five samples in terms of curve shape and magnitude of hysteresis. The hysteresis is attributed to the pore structure of each of the samples (all of which have mesopores or macropores) and the phenomenon that the vapor pressure of an adsorbate in a pore decreases as the pore size (i.e. radius r) decreases (Kelvin equation):

$$P/Po = \exp(-2V\gamma \cos\theta/rRT) \qquad 6)$$

According to the Ink Bottle Hypothesis, which pictures a pore as having an entrance channel of smaller radius than its bulk volume, adsorption occurs in a pore when the CO_2 relative pressure rises to equal the vapor pressure corresponding to the radius of the "bulk" pore. However, on the desorption curve, as the pressure is reduced, the corresponding desorption does not occur until the pressure reaches a lower value, corresponding to the lower vapor pressure present in the "bottle-neck" of smaller radius, because a meniscus of adsorbate has formed in the bottle-neck. Thus, for a given amount adsorbed, the desorption isotherm lies to the left (i.e. toward lower pressures) of the adsorption isotherm.

This phenomenon also explains the general shape (i.e. concave upward) of the isotherms and the observed change in shape from concave to sigmoidal as the temperature is increased (Figures 1 and 2). Generally, the specific amount adsorbed increases as temperature increases, indicating that some chemisorption (as well as physical adsorption) is present at higher temperatures. The pressure at which the maximum slope of the isotherm occurs decreases as

temperature increases, indicating that the "effective pore radius" decreases: As pore radius decreases, vapor pressure decreases, so that adsorption can occur at lower relative CO_2 pressures; and an increase in temperature increases the vapor pressure in a given pore radius. Since each solid sample is characterized by a pore size distribution, adsorption occurs in different parts of the sample at different pressures, as reflected by the isotherm's shape at equilibrium. The slope is a measure of the increment of adsorption that occurs in response to an increment of CO_2 relative pressure, and thus measures the frequency of pores with a given radius. Thus, for a given sample, it is observed that the adsorption isotherm becomes more sigmoidal (i.e. more like a BET isotherm) as temperature increases: the pressure of maximum adsorption shifts to lower values, indicating that the vapor pressure and "effective" pore size both decrease.

A final observation of this experiment is that the specific amount adsorbed per unit weight of adsorbent increases as particle size decreases (or specific surface area increases) among the six samples and among the three Lignite samples of different particle size. At 20°C and 100% relative pressure, Pyrite showed the lowest specific amount adsorbed (about 0.09 g/g); and 400-mesh Lignite showed the highest amount (about 0.12 g/g). Generally, the order of the amount adsorbed corresponded to the order of specific surface area (or inverse order of particle size) for the six samples at a given temperature and CO_2 pressure (Tables 2 and 3). Finally, these results (per unit weight of adsorbent) are divided by the specific surface area of the corresponding sample (from the BET results) to obtain the adsorption isotherms per unit surface area of adsorbent at each temperature and CO_2 pressure. It is found that this specific amount adsorbed varied very little amoung the six samples, indicating that the intrinsic nature (i.e. hydrophobicity) of the sample has a very little effect on its adsorption properties. Thus, it is concluded that adsorption at equilibrium is an extensive property (i.e. depends on the amount of sample, or the availibility of surface area).

The final experiment involves measuring the equilibrium advancing contact angles and several types of interfacial tension as a function of sample, CO_2 pressure, temperature, and CO_2 phase. As before, each parameter is varied independently to isolate its effect on the interfacial properties. Four temperatures (10, 15, 20, and 25°C) and CO_2 relative pressure in increments of 25% (from zero to 100%) are tested; and $CO_2(g)$ and $CO_2(l)$ are used separately. In

the pendant drop experiment, it is found that the liquid-vapor interfacial tension (Table 4) decreases dramatically as pressure increases (i.e. at 25°C: from 72.03 dyne/cm at 0% to 33.01 dyne/cm at 100% relative CO_2 pressure), decreases slightly with temperature (i.e. at 100% relative pressure: from 35.38 dyne/cm at 10°C to 33.01 dyne/cm at 25°C), and decreases significantly as a switch is made from $CO_2(g)$ to $CO_2(l)$. For example, at 10°C, the tension decreases from 35.38 to 27.09 dyne/cm when the switch is made to $CO_2(l)$. These changes are reflected by the changes in the pendant drop's equilibrium physical dimensions (De, Ds, S = De/Ds, and Hs = f(S)) and by the change in density difference ($p_2 - p_1$) between the water drop and surrounding CO_2 medium. The physical picture is explained mathematically by Laplace's equation of capillarity and the criteria that the surface and gravitational forces are equal at equilibrium:

$$P'' - P' = \gamma \cos\theta (1/r_1 - 1/r_2) = 2\gamma \cos\theta / r \qquad 7)$$

$$Fg = mg = pVg = pg(4/3\,\pi r^3) = 2\pi r \gamma = Fs \qquad 8)$$

Recognizing the nature of curved surfaces, an increase in pressure or temperature decreases the pressure difference across the curved interface and thus decreases the surface force and hence the interfacial tension. As the pendant drop grows in radius, gravitational force increases more rapidly than the surface force. Because of the depressed surface force, the drop has smaller dimensions and a lower interfacial tension at equilibrium, as a result of a pressure or temperature increase. When the switch is made from $CO_2(g)$ to $CO_2(l)$, the density difference between the water drop and CO_2 phase decreases; $CO_2(l)$ has a density comparable to (but still less than) that of water (0.80 vs. 1.00 g/cm^3 at 25°C), as compared to $CO_2(g)$. According to Andreas, Hauser, and Tucker, the interfacial tension in this two-phase system is proportional to this density difference:

$$\gamma = g\,(p_2 - p_1)\,De^2/Hs \qquad 9)$$

Thus, a decrease in interfacial tension is expected when a switch is made from $CO_2(g)$ to $CO_2(l)$ at 100% CO_2 relative pressure.

In the sessile drop experiment, the equilibrium advancing contact angle is measured versus CO_2 pressure, temperature, and CO_2 phase. Generally, it is found that the contact angle increases when: CO_2 pressure increases, temperature decreases, or $CO_2(l)$ is used. These trends can similarly be explained by the above argument, Laplace's equation, and the equilibration of surface and gravity forces at equilibrium. According to Padday, a sessile drop is in equilibrium when the top is flat and at maximum height. For most samples, except the hydrophobic Graphite Powder, the contact angles at all temperatures are

essentially zero at relative pressures less than 50%, indicating a completely wettable system. Thus, the optimal system conditions for enhancing incomplete wetting for a given sample are a high pressure (preferably 100%), low temperature, and the use of $CO_2(l)$ as the surrounding medium. It is also found that, among the Lignite samples, contact angle increases when particle size decreases. At 10°C and 100% relative pressure, the average contact angle values for 35-mesh, 200-mesh, and 400-mesh Lignite are, respectively: 87.50°, 96.25°, and 107.50° with $CO_2(g)$; and 103.75°, 117.50°, and 128.75° with $CO_2(l)$.

Furthermore, among all six samples, no correlation is found between particle size and equilibrium contact angle. Graphite Powder, known to be hydrophobic in nature, is found to have the largest overall contact angle values, ranging (at 10°C) from 90.00° at 25% to 147.50° at 100% with $CO_2(g)$, and 152.50° with $CO_2(l)$. Thus, Graphite Powder is the most incompletely wettable sample. Pyrite shows more intermediate contact angle values, its highest value being 95.00° at 10°C with $CO_2(l)$, and is found to have the second lowest average contact angle at a given temperature, CO_2 pressure, and CO_2 phase. The sample with the lowest average value (i.e. the most hydrophilic sample) is the clay-like Kaolin, which shows a zero contact angle (i.e. complete wetting) even up to 100% relative pressure with $CO_2(g)$. Its largest value is 30.00°, at 10°C with $CO_2(l)$. Thus, the general order of wetting is, from complete to incomplete: Kaolin, Pyrite, Lignite (35-mesh, 200-mesh, 400-mesh), and Graphite Powder, because the magnitude of the equilibrium advancing contact angle is inversely related to the tendency of a three-phase system toward complete wetting. Thus, contact angle is found to be an intensive property, because it depends not only on particle size (or specific surface area) but also on the sample's intrinsic nature (i.e. hydrophobicity).

Using the two-phase equilibrium interfacial tension and contact angle data, the solid-vapor and solid-liquid interfacial tension are calculated using Equations 1 and 2. It is generally found that the solid-vapor tension first decreases and then increases with pressure. This is explained by the fact that complete wetting (i.e. a zero contact angle) is predominant at the lower relative pressures, and film pressure is still negligible; thus, the solid-vapor tension is first constant or decreasesightly. At higher pressures, incomplete wetting sets in; and film pressure (i.e. the presence of an adsorbed vapor film on the solid surface) becomes significant. Thus, based on the interfacial tension of a clean, pure solid in a vacuum, the solid-vapor tension increases with pressure to reflect the

film pressure increase. Generally, as incomplete wetting becomes significant, the solid-vapor tension increases. This argument also explains the observation that this tension increases when the switch is made from $CO_2(g)$ to $CO_2(l)$ at a given temperature.

This tension is also found to be relatively constant with temperature as a result of the cancellation effect of temperature on contact angle and the liquid-vapor tension in Young's equation: As temperature increases, θ decreases, cos θ increases, and the liquid-vapor tension decreases; so the product $\gamma_{lv} \cos\theta$ is essentially constant with temperature. Among the six samples, the solid-vapor tension is lowest for Kaolin (about 88.0 dyne/cm with $CO_2(l)$) and highest for Graphite Powder (about 107.0 dyne/cm with $CO_2(l)$). The order of magnitude for this tension (averaged over the four temperatures) is, in increasing order: Kaolin (88.0 dyne/cm), Pyrite (99.0 dyne/cm), 35-mesh Lignite (101.0 dyne/cm), 200-mesh Lignite (102.5 dyne/cm), 400-mesh Lignite (104.5 dyne/cm), and Graphite Powder (107.0 dyne/cm). This is the same order of increasing contact angle and of decreasing wettability. Thus, among the Lignite samples, this tension decreases as particle size increases. Like the contact angle, the solid-vapor interfacial tension is an intrinsic property, because it depends on contact angle.

Another interfacial tension that is calculated is the solid-liquid tension, which is found to increase with CO_2 pressure continuously (because of the corresponding increase in contact angle and decrease in the system's wetting tensency, and the insignificant effect of film pressure on this tension), remain constant with temperature (because the term $\gamma_{lv} \cos\theta$ is essentially constant with temperature), and increases when $CO_2(l)$ is used (because of the enhancement of incomplete wetting). It is observed among the Lignite samples that the solid-liquid tension decreases as particle size increases. Among the six samples, the order of magnitude for this tension parallels that for solid-vapor tension (reflecting the trend toward incomplete wetting) and is, in increasing order (averaged over the four temperatures): Kaolin (63.0 dyne/cm), Pyrite (98.0 dyne/cm), 35-mesh Lignite (106.0 dyne/cm), 200-mesh Lignite (111.0 dyne/cm), 400-mesh Lignite (120.0 dyne/cm) and Graphite Powder (128.0 dyne/cm). Thus, solid-liquid tension is an intensive property, reflecting hydrophobicities as well as particle size.

The main conclusion obtained from this project is the optimization of reaction conditions to enhance the system's tendency toward incomplete wetting and thus enhance the

potential for separation. Graphite Powder has the highest tendency; and, among the Lignite samples, 400-mesh Lignite has the highest incomplete wetting tendency. For a given sample, incomplete wetting is favored at high relative CO_2 pressures, low temperatures, and the presence of $CO_2(l)$. It is found that, while equilibrium adsorption is an extensive property (i.e. depends only on particle size and thus available specific surface area), the contact angle and interfacial tensions are intensive properties. From the preliminary results, an inverse relation exists between particle size and specific surface area of a powdered sample; and these results make possible and more complete the study of the adsorption and interfacial properties of the six coal minerals.

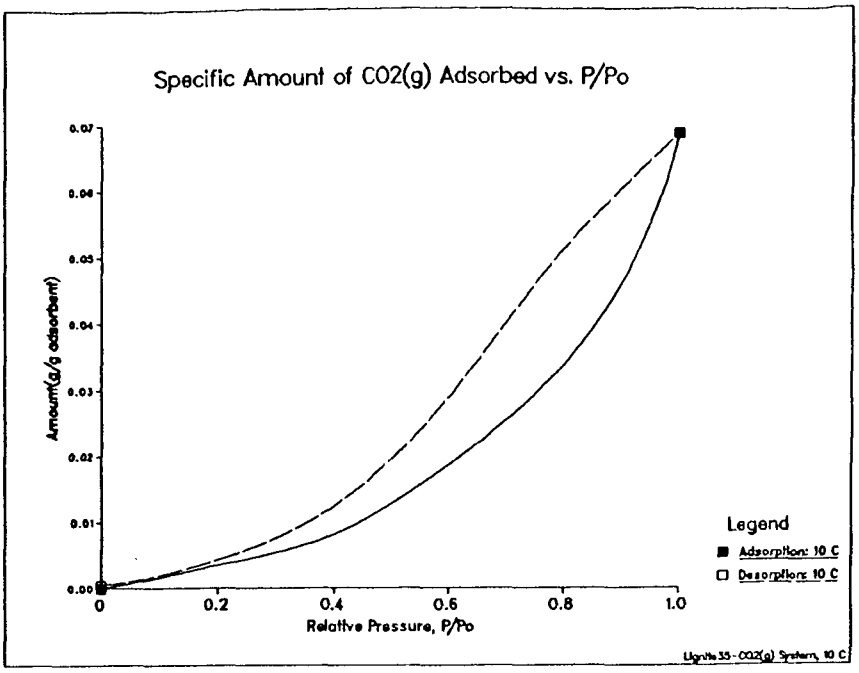

Figure 1 Adsorption and Desorption Isotherms vs. CO_2 Pressure for 35-Mesh Lignite at 10° C

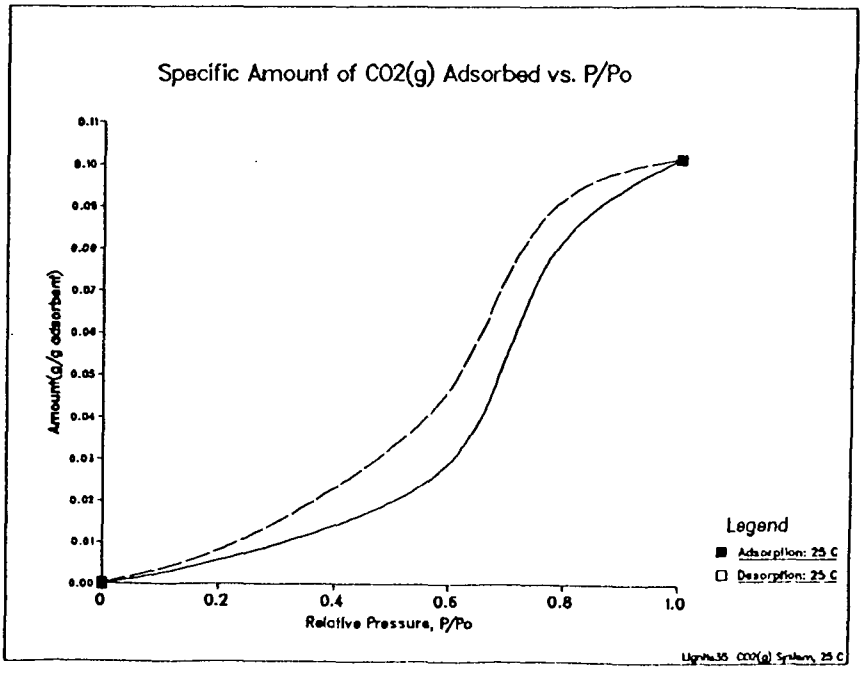

Figure 2 Adsorption and Desorption Isotherms vs. CO_2 Pressure for 35-Mesh Lignite at 25° C

Table 1

Average Characteristic Diameters and Specific Surface Areas of Powdered Particle Samples of Lignite (35-, 200-, and 400-Mesh), Graphite Powder, Kaolin, and Pyrite

Sample	Length Diameter (um)	Volume Diameter (um)	Surface Diameter (um)	Surface-Volume Diameter	Weight Diameter (um)	Specific Surface Area(m^2/g)
35-Mesh Lignite	9.2	17.6	12.8	33.7	54.2	17.8
200-Mesh Lignite	7.6	14.5	10.3	28.9	56.2	19.9
400-Mesh Lignite	7.5	12.4	9.7	20.6	31.1	21.1
Graphite Powder	8.8	16.2	12.0	29.8	46.0	18.1
Kaolin	9.1	15.1	11.6	25.8	44.5	18.9
Pyrite	16.9	30.6	23.5	52.7	72.5	17.4

Table 2

Specific Amount of CO_2 Adsorbed (per unit weight of adsorbent) Along the Adsorption Isotherm for Lignite (35-, 200-, and 400-Mesh) (g/g adsorbent)

35-Mesh Lignite

Temp.(°C)	Relative Pressure (P/Po)					
	0.00	0.20	0.40	0.60	0.80	1.00
10	0.00	0.00350	0.00817	0.01854	0.03367	0.06876
15	0.00	0.00403	0.01094	0.02007	0.05378	0.08830
20	0.00	0.00538	0.01205	0.02723	0.07121	0.09384
25	0.00	0.00568	0.01403	0.02895	0.08239	0.10107

200-Mesh Lignite

Temp.(°C)	Relative Pressure (P/Po)					
	0.00	0.20	0.40	0.60	0.80	1.00
10	0.00	0.00411	0.00928	0.02012	0.03630	0.07286
15	0.00	0.00432	0.01119	0.02187	0.05635	0.09600
20	0.00	0.00574	0.01303	0.03114	0.07820	0.09905
25	0.00	0.00613	0.01635	0.03278	0.08916	0.10980

400-Mesh Lignite

Temp.(°C)	Relative Pressure (P/Po)					
	0.00	0.20	0.40	0.60	0.80	1.00
10	0.00	0.00426	0.00980	0.02140	0.03810	0.07622
15	0.00	0.00471	0.01259	0.02303	0.05957	0.09908
20	0.00	0.00591	0.01376	0.03172	0.10813	0.11794
25	0.00	0.00648	0.01790	0.03359	0.09855	0.12426

Table j

Specific Amount of CO_2 Adsorbed Along the Adsorption Isotherm for Graphite Powder, Kaolin, and Pyrite (g/g adsorbent)

Graphite Powder

Temp.('C)	Relative Pressure (P/Po)					
	0.00	0.20	0.40	0.60	0.80	1.00
10	0.00	0.00368	0.00878	0.01891	0.03415	0.06957
15	0.00	0.00394	0.01081	0.02013	0.05395	0.09038
20	0.00	0.00532	0.01198	0.02711	0.06940	0.09678
25	0.00	0.00563	0.01411	0.02934	0.08481	0.10537

Kaolin

Temp.('C)	Relative Pressure (P/Po)					
	0.00	0.20	0.40	0.60	0.80	1.00
10	0.00	0.00382	0.00891	0.01990	0.03467	0.07188
15	0.00	0.00415	0.01121	0.02096	0.05380	0.09160
20	0.00	0.00548	0.01232	0.02751	0.08730	0.10611
25	0.00	0.00571	0.01601	0.03058	0.09110	0.11245

Pyrite

Temp.('C)	Relative Preesure (P/Po)					
	0.00	0.20	0.40	0.60	0.80	1.00
10	0.00	0.00340	0.00780	0.01816	0.03319	0.06840
15	0.00	0.00376	0.01070	0.01959	0.05361	0.08719
20	0.00	0.00520	0.01170	0.02695	0.06488	0.08843
25	0.00	0.00551	0.01343	0.02789	0.07391	0.09568

Table 4

Equilibrium Liquid-Vapor and Liquid-Liquid Interfacial Tensions from the Pendant Drop Method (dyne/cm)

Liquid-Vapor Interfacial Tension

Temp.('C)	Relative Pressure (P/Po)					
	0.00	0.25	0.50	0.75	1.00 CO_2(g)	1.00 CO_2(l)*
10	74.27	63.84	53.59	43.42	35.38	27.09
15	73.77	63.51	52.42	43.91	35.07	26.42
20	72.73	61.89	52.87	44.15	34.33	25.37
25	72.03	61.39	51.84	43.40	33.01	23.32

Work of Cohesion (twice the interfacial tension)

Temp.('C)	Relative Pressure (P/Po)					
	0.00	0.25	0.50	0.75	1.00 CO_2(g)	1.00 CO_2(l)
10	148.54	127.67	107.17	86.85	70.76	54.19
15	147.54	127.02	104.83	87.83	70.13	52.84
20	145.47	123.78	105.74	88.30	68.66	50.74
25	144.07	122.78	103.69	86.81	61.40	47.65

* The first four columns tabulate the liquid-vapor interfacial tensions, whereas the last column lists the liquid-liquid interfacial tensions. They are distinguished by the phase of CO_2 surrounding the pendant drop.